ELSEVIER

Polymer 40 (1999) 5553–5565

polymer

Effect of draw ratio and temperature on the strain-induced crystallization of poly (ethylene terephthalate) at fast draw rates

A. Mahendrasingam[a], C. Martin[a], W. Fuller[a,*], D.J. Blundell[b], R.J. Oldman[b], J.L. Harvie[c], D.H. MacKerron[c], C. Riekel[d], P. Engström[d]

[a]*Department of Physics, Keele University, Staffordshire ST5 5BG, UK*
[b]*ICI Research and Technology Centre, PO Box 90, Wilton, Middlesbrough, Cleveland TS90 8JE, UK*
[c]*DuPont UK Ltd, PO Box 2002, Wilton, Middlesbrough, Cleveland TS90 8JS, UK*
[d]*ESRF, BP 220, F-38043 Grenoble Cedex, France*

Received 5 December 1997; received in revised form 4 June 1998; accepted 14 October 1998

Abstract

Wide angle X-ray scattering (WAXS) data recorded during the drawing of poly(ethylene terephthalate) (PET) under industrial processing conditions was analysed in terms of changes in the degree of polymer orientation and crystallinity over a wide range of draw temperatures and draw ratios. The actual draw rate and draw ratio at the region in the specimen from which X-ray data was recorded was determined independently with high consistency by direct video observation of strain and total X-ray scattering. In contrast to previous claims, the start of strain-induced crystallization coincided with the end of draw within the 40 ms time-resolution of the investigation. Crystallization has been shown to follow first order kinetics and the rate constant was determined over a range of temperatures from 85°C–125°C. Above 125°C little orientation is observed with no evidence of strain-induced crystallization. A detailed determination was made of the critical value of draw ratio below which strain-induced crystallization does not occur and where a relaxation in molecular orientation is observed after the extension process. The implications of these experimental observations for existing theory of strain-induced polymer crystallization are discussed.

Keywords: PET; Crystallization; X-ray diffraction

1. Introduction

The exploitation of poly(ethylene terephthalate) (PET) as a polymer material typically involves mechanical deformation at elevated temperatures close to its T_g. Such processing can have major effects on the degree of polymer orientation and crystallinity and hence on the physical properties of the material. X-ray diffraction provides one of the most powerful techniques for characterizing polymer orientation and crystallinity and hence for exploring the relationship between industrial processing conditions and the properties of the finished artefact. The increasing availability of synchrotron radiation sources during the last decade with a brilliance in the X-ray region many orders of magnitude greater than conventional laboratory sources has dramatically extended the power of diffraction techniques for investigating polymer conformation and organization and in particular the variation of these characterisitics on timescales comparable to those of industrial processing. The information obtainable from these techniques is of fundamental importance in understanding the strain-induced crystallization process which occurs when polymers such as PET are oriented close to their T_g and on which there has been very little information to date.

This article is part of a systematic extension of our earlier work [1] and focuses on the effect of draw ratio and draw temperature on the development of orientation and crystallinity when a sheet of PET is oriented at fast uniaxial draw rates i.e., $\sim 10\ s^{-1}$. In particular the article follows up two issues raised by unexpected observations in our previous work. The first was that the crystallization process was found not to start until after the completion of the drawing processs, which in the previous work occured at final draw ratios $\sim 4:1$. This contrasts with other detailed studies on the orientation of PET such as that of Salem [2] and of Le Bourvellec and Monnerie [3] who carried out interrupted draw experiments over a range of draw rates. In these cases the level of crystallinity was deduced from specimens after they had been quenched to room temperature rather than by the real-time observations made in our synchrotron

* Corresponding author. Tel.: 01782 583326; fax: 01782 711093.

0032-3861/99/$ - see front matter
PII: S0032-3861(98)00770-8

studies, where two-dimensional wide angle diffraction patterns could be recorded with exposures as short as 40 ms. The earlier experiments using quenched samples led to an interpretation in which it was proposed that distinct stages in the crystallization process occurred during the draw at distinct points of the stress–strain curve and in particular that the onset of crystallization occurred at draw ratios of $\sim 2:1$. Although our synchrotron data has shown that, at least for fast draw rates, deductions from interrupted draw can be misleading, these earlier analyses do emphasize the need to explore whether there are critical points in the drawing process which may be associated with marked changes in polymer behaviour in response to mechanical stress. The second issue arising from our previous synchrotron studies was that the crystallization rate was found to be insensitive to temperature and also appeared to follow the kinetics of a first order transformation process in which the crystallinity levelled off to its final value exponentially with time. This is in contrast with the crystallization of unoriented PET which usually approximately follows Avrami kinetics with an exponent $n \sim 3$, where the rate would be expected to vary by three orders of magnitude over the temperature range investigated in our experiments. We speculated [1] that the temperature insensitivity we observed could be a consequence of the strain-induced crystallization involving local segment reorientation processes and did not depend on main chain motions where there is a strong temperature dependence on T_g.

In order to address these issues, experiments were carried out at the same high draw rate but over a wider range of temperature from 85°C–140°C in order to investigate in more detail the nature of the strain-induced crystallization kinetics. Also, for a draw temperature of 90°C, identical drawing experiments were performed for a series of final draw ratios ranging from $\sim 4.0:1$ down to $\sim 2.0:1$, in order to ascertain whether there is a critical lower draw ratio for the crystallization process. Taken together these new observations demonstrate that the strain-induced crystallization process occurring at fast draw rates requires a critical degree of chain segment orientation which depends on both temperature and draw ratio.

2. Experimental

Wide angle X-ray diffraction data was recorded on beamline ID13 at the European Synchrotron Radiation Facility (ESRF), Grenoble using a purpose designed X-ray diffraction camera constructed in the Keele Physics Department workshops [4]. It consisted of a 150 mm × 150 mm × 150 mm oven made of insulated aluminium plates of which three sides were made to be interchangeable so that it was possible to exchange sides depending on the particular application. This allowed the position of a viewing port in which a video camera was mounted to be varied according to the overall size and shape of the specimen being studied. The oven was heated electrically by elements mounted on the top and bottom of its interior and the temperature was kept uniform by the use of an air circulating fan. The temperature of the oven could be controlled to within 1°C and the maximum temperature available was ~ 350°C. The sample of PET was clamped between two jaws attached to stepper motors which allowed uniaxial bidirectional drawing at an overall rate of $\sim 13\ s^{-1}$. There are small variations in the time of the start of draw as a result of small differences of initial slack in the clamped sample.

Beamline ID13 is based on a low-β undulator and uses a channel-cut silicon monochromator and ellipsoidal mirror combination to produce a low divergence beam $\sim 40\ \mu m \times 20\ \mu m$ in cross section with a wavelength of 0.92 Å. This beam is smaller in area by a factor of ~ 10 than is achievable, without substantial loss of incident beam intensity, on the second generation synchrotron radiation sources available prior to the commissioning of the ESRF. This higher brilliance is of particular importance for studies of this kind because it allows structural variation across the specimen to be characterized with a correspondingly higher degree of spatial resolution. Diffraction patterns were recorded using a Photonics Science CCD detector with a sensitive area 92 mm × 69 mm and an effective pixel area of 120 μm × 120 μm. The specimen to detector distance could be as small as 6 cm. At this specimen to detector distance d spacings from ~ 15 Å to ~ 1.5 Å could be recorded. Diffraction patterns were recorded with exposure times of 40 ms. Over this period, the pattern was integrated within the detector before being digitized by a Synoptic i860 frame grabber within an 8-bit word. Up to 124 frames could be recorded "end-to-end" with essentially no dead-time between frames before the memory of the frame grabber was full, at which point they were downloaded through a SCSI interface to a Pentium PC. The variation in the overall size and shape of the specimen during drawing was also recorded as a series of 40 ms frames whose collection by the video recorder was accurately synchronized with the recording of the variation in the X-ray diffraction.

Specimens ~ 10 mm wide were cut from a sheet of ~ 840 μm thick cast film of amorphous unoriented PET. The polymer had a number average molecular weight of ~ 20,000. Ink reference stripes were drawn with a separation of 1 mm on the specimen at right angles to the draw direction to enable the degree of extension at the point in the specimen from where the diffraction data was recorded to be calculated from the video camera image. Independent estimates of draw ratio were obtained by assuming that the total detector count in each frame was proportional to the amount of polymer material scattering when the frame was recorded and hence was proportional to the thickness of the specimen at the precise region of the specimen from which the diffraction was recorded. There is a high degree of correspondence between the two methods for periods of the draw prior to crystallization. The method based on total detector count had the advantage that it could be applied automatically

Table 1
Comparison of crystallinity, the crystallization rate and the average draw rate of the PET samples drawn at various draw temperatures and draw ratios

Draw temperature (°C)	Overall final draw ratio	Final crystallinity from density	Average draw rate (s^{-1})	Crystallisation rate (s^{-1})
85	4.0	0.263	14.7	6.9
90	4.0	0.260	13.5	7.9
95	3.5	0.256	10.1	8.9
100	3.7	0.269	9.3	8.8
110	3.7	0.308	9.5	8.5
90	4.0	0.263	13.5	7.9
90	3.1	0.212	8.2	5.5
90	2.6	0.203	6.3	2.0
90	2.2	0.109	5.8	0.4

without additional measurement of the variation in the separation of the reference stripes drawn on the specimen. This method also gives a more precise determination of the end of local draw at the point monitored by X-ray beam.

The specimen was mounted in the jaws of the camera with a 10 mm gauge length. The control of the stepper motors of the camera were set to move the jaws apart at a rate of 133 mm s^{-1}. The specimens were heated in the camera to 90°C and allowed to equilibrate for 2 min. They were then drawn to various final draw ratios by stopping the motors after various numbers of steps.

Intensity distributions were corrected for background effects by pixel-by-pixel subtraction of "blanks" recorded in the absence of the specimen immediately after each draw. The density of each specimen following drawing was measured and the percent crystallinity estimated assuming a two phase model with a crystal density of 1.4570 $g.ml^{-1}$ and an amorphous density of 1.3350 $g.ml^{-1}$. These estimated crystallinities are listed in Table 1 together with the corresponding draw ratios.

Experiments of this type generate very large amounts of data whose analysis is only made feasible on an acceptable time scale by the use of semi-automatic techniques. A suite of programmes was developed which allows frame manipulation and objective analysis of the diffraction patterns to give a quantitative measure of the development of crystallinity, orientation and the local draw ratio at the region of the specimen from where the diffraction data was recorded. As a crucial part of these analyses involves the estimation of an appropriate background level and the differentiation of oriented crystalline and amorphous diffraction, a highly critical approach to the results was adopted. We were however extremely reassured to find that the curve fitting procedures used were extremely "well behaved" with the results from successive frames exhibiting a high degree of self-consistency. Nevertheless, as is indicated in the following discussions, these analyses should be seen primarily as providing measures of relative changes in the degree of orientation and crystallinity rather than absolute values.

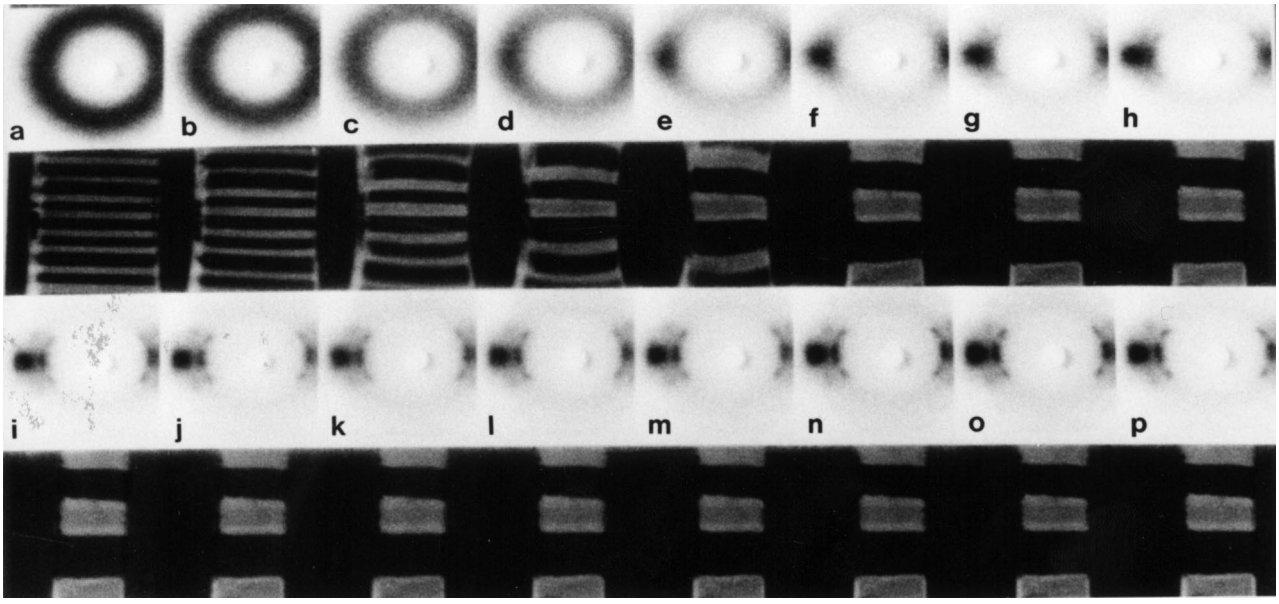

Fig. 1. Selected X-ray diffraction patterns and video images of a PET sample drawn at 90°C with overall draw ratio 4.0:1. Diffraction patterns (a–o) corresponding to frames (1–15) and p corresponding to frame 124. Each frame was recorded in 40 ms with no "dead-time" between frames.

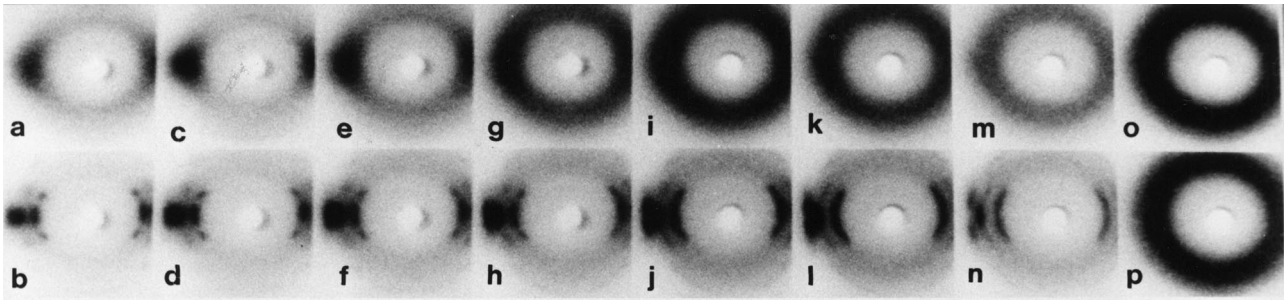

Fig. 2. X-ray diffraction patterns of the PET sample drawn at 85°C (a, b), 90°C (c, d), 95°C (e, f), 100°C (g, h), 110°C (i, j), 120°C (k, l), 125°C (m, n) and 130°C (o, p) (i) Diffraction patterns in the top row of the figure (i.e., a, c, e, g, i, k, m and o) corresponding to end of the draw but before the onset of crystallisation. (ii) Diffraction patterns in the bottom row of the figure (i.e., b, d, f, h, j, l, n and p) corresponding to final frame (124) of the experiment.

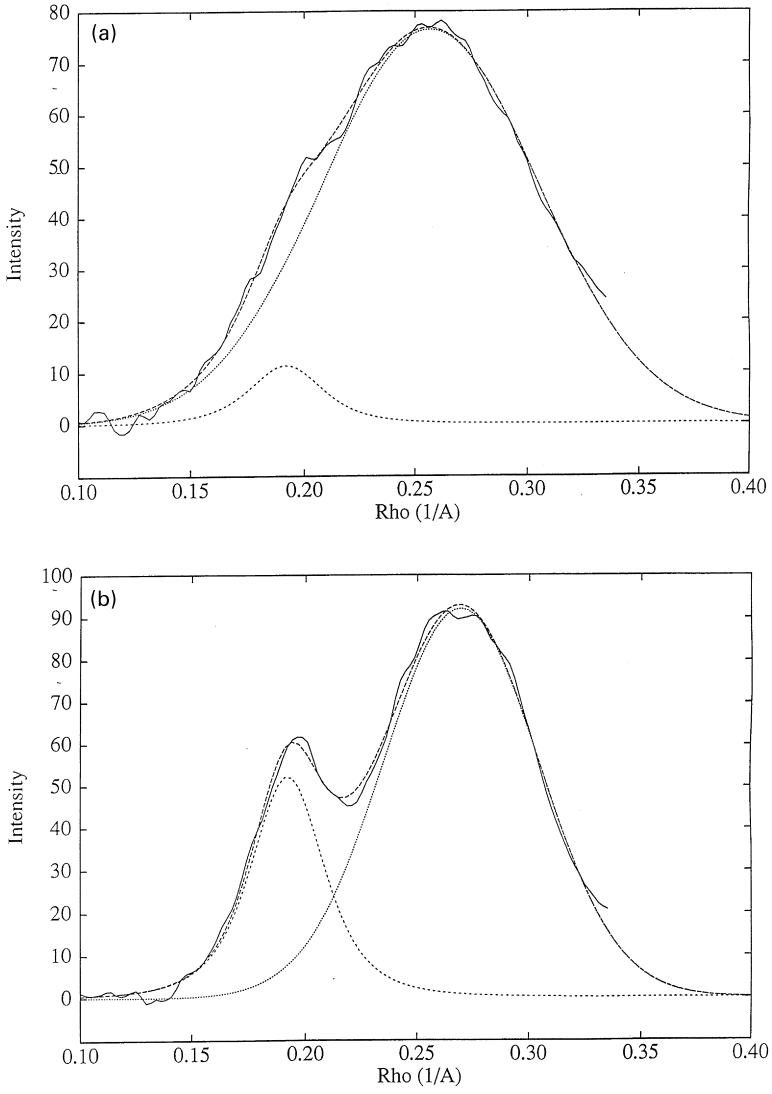

Fig. 3. Examples from the experiment illustrated in Fig. 1 showing the fitting of a Pearson VII function to the region of the (010) reflection of the equatorial scan from (a) frame 7 (b) frame 124. The continuous line in both figures is the original scan and the three doted lines represent the two contributing components identified in the least squares analysis and their sum.

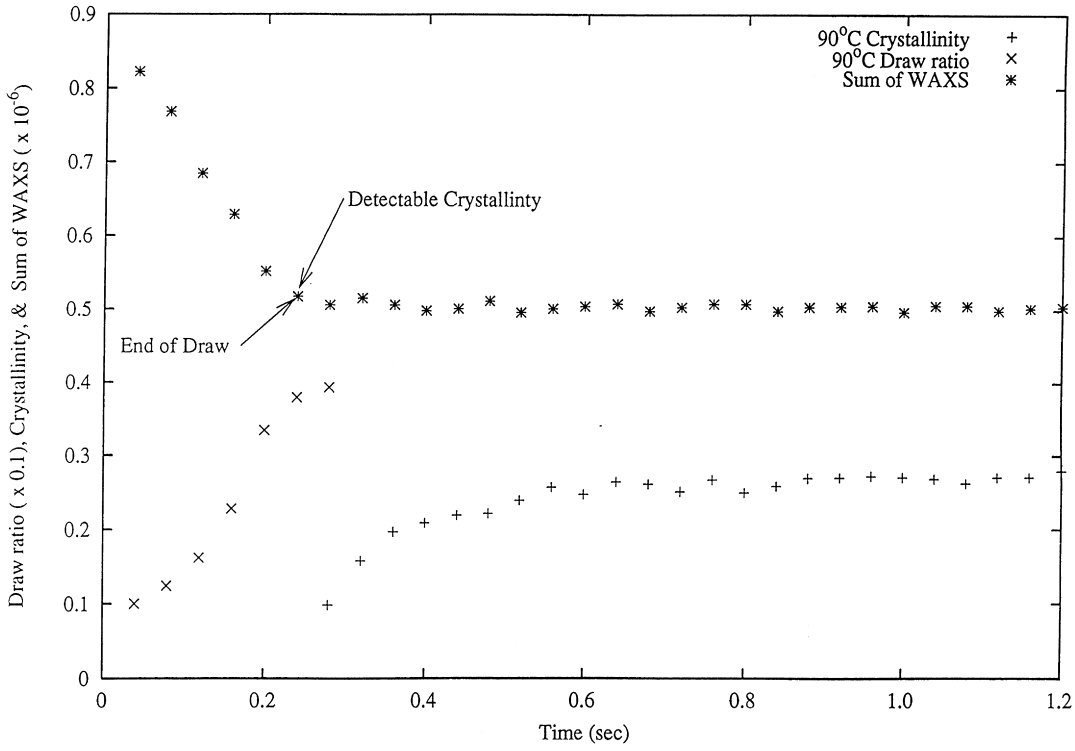

Fig. 4. Plot of the variation in draw ratio and crystallinity calculated from the sequence of X-ray diffraction patterns of the PET sample recorded during the drawing at 90°C to a final draw ratio 4:1. The arrow indicates first frame with detectable crystallinity and end of draw.

3. Results

An example of the type of data obtained in the studies analyzed in this article is shown in Fig. 1 for the data set at 90°C with a final draw ratio of 4.0:1. This shows a composite image of an array of X-ray patterns selected from the 124 recorded during the draw and the corresponding video images of the sample. The initial pattern (Frame 1) is an unoriented amorphous halo. As drawing proceeds there is a gradual intensification of the halo at the equator leading to diffuse equatorial lobes characteristic of a highly oriented, non-crystalline structure (Frame 7) within which sharp diffraction spots characteristic of a highly oriented crystalline phase then develop (Frames 8–124). Visual comparison of this variation with that of the video image of the sample shows that the crystalline spots do not begin to develop until after the extension process has stopped.

There are variations in the appearance of the diffraction patterns between the various draw experiments, particularly at the highest temperature. This is illustrated in Fig. 2 which shows for each temperature the final frame (Frame 124) and the frame corresponding to the point at the end of the mechanical draw but before significant crystallization occurs. With increasing temperature, the final frame shows a systematic change in the relative intensities and the azimuthal positions of the crystalline spots. The change in the relative intensities is similar to that seen previously by other authors [5] with a progressive increase in the relative intensity of the (100) reflection consistent with a reduction in the preferential alignment of the (100) planes parallel with the plane of the film. Some of the spots are progressively split to form doublets above and below the equator indicating an increase in a tilt of the crystal *c*-axis relative to the draw axis [6]. The corresponding frames at the end of the mechanical draw show a progressive decrease in the intensity of the diffuse equatorial lobes indicating a decrease in molecular orientation so that by 130°C there are no longer any indications of orientation in the pattern. These changes are consistent with the increased molecular relaxation characteristic of higher temperatures competing with the tendency towards orientation as a result of mechanical stress. The absence of oriented crystalline growth at 130°C suggests that, by this temperature, the net molecular orientation has fallen below the level necessary for strain-induced crystallinity to be initiated.

The development of crystallinity was followed by fitting radial traces of the variation in intensity across the equator of successive frames by a family of Pearson VII [7] functions to represent overlapping crystalline reflections and oriented and non-oriented diffuse diffraction. In all cases it was possible to isolate a single equatorial reflection that could be fitted with a single Pearson VII function with the remaining diffraction represented by a broad Pearson VII peak. This analysis is illustrated for a frame close to the onset of crystallinity in Fig. 3a and one recorded at the end of the crystallization process in Fig. 3b. It is important

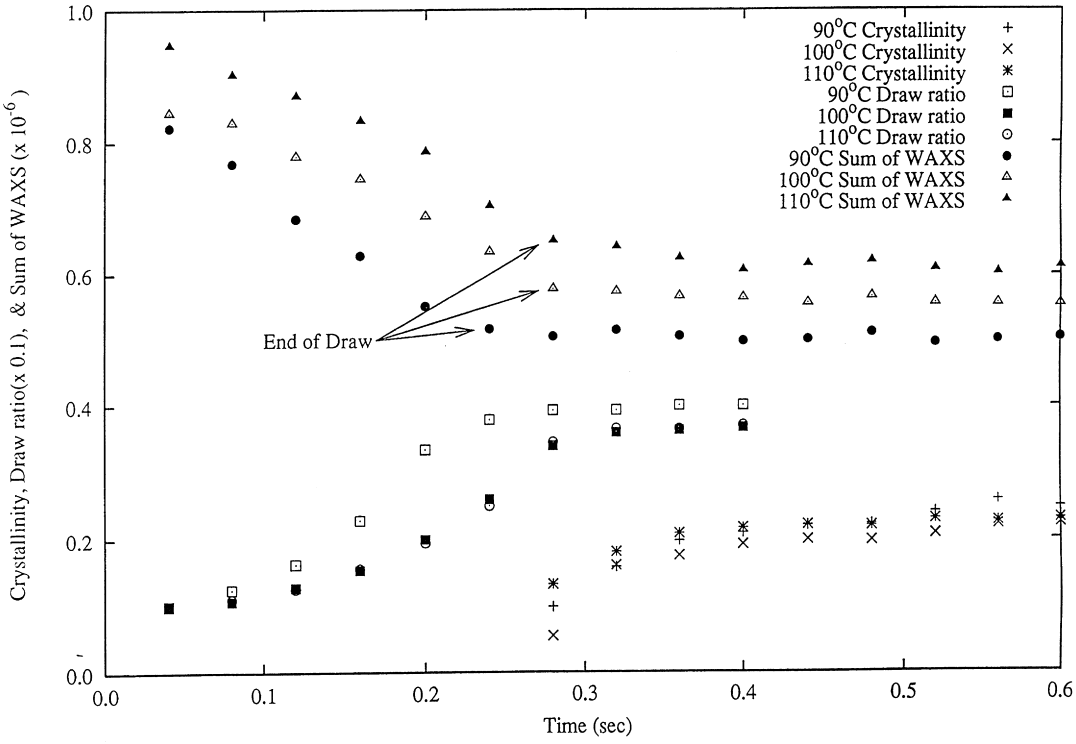

Fig. 5. Plot of the variation in draw ratio and crystallinity calculated from the sequence of X-ray diffraction patterns of PET samples recorded during the drawing at 90°C, 100°C and 110°C for final draw ratio of 4:1.

to emphasize that in this analysis the positions in reciprocal space of the two peaks were not constrained and the refined position of the crystalline peak was that to be expected for the (010) reflection in a highly crystalline oriented pattern of PET. Fig. 4 illustrates the application of this approach to the frames in Fig. 2 from the onset of crystallization onwards. This figure shows both measured draw ratio and total intensity and illustrates the validity of the method of measuring the draw ratio at point of the beam. The arrows indicates the end of draw and the first frame where there is detectable crystallinity. The area of the (010) peak as represented in this analysis provides a relative measure of how crystallinity is evolving with time after the completion of the draw. Fig. 5 shows a plot of peak area as a function of frame number for different temperatures during the initial ~ 1 s of the experiments. Also plotted are the draw ratios derived from the corresponding video images and total X-ray count for the initial frames up to the end of the extension process. These plots confirm the visual impression of Fig. 2 that the crystallization process starts close to the point of final extension with the degree of crystallization levelling off asymptotically to a final value. It should be noted that whilst the variation in peak area during a draw gives a meaningful measure of relative levels of crystallinity during a draw, much more caution is required in treating these areas as measures of absolute values of crystallinity and in particular as a measure of differences in the final levels of crystallinity in different draws.

The development of orientation was followed by analyzing azimuthal scans of successive frames at a reciprocal space distance of 0.28 $\mathring{A}^{-1}$. This corresponds to the position of the maximum in the equatorial scan of the diffuse diffraction at the onset of crystallization. An example of an azimuthal scan is illustrated in Fig. 6a where the peak in the scan is equatorial. The scans were analyzed as shown in Fig. 6b by fitting them with a Pearson VII function plus a linear background. For simplicity the curves were characterized by calculating the orientation order parameter $< P_2(\cos\theta) >$ of the Pearson VII component of the fit using the expression derived by Lovell and Mitchell [8]. This is a convenient way of following the development of non-crystalline orientation during the mechanical drawing process. Fig. 7 illustrates the development of this orientation parameter for the frames in Fig. 2 as well as from corresponding frames at other temperatures. The arrow on the plot indicates the end of draw derived from the total intensities. It is interesting to note that the value of the orientation parameter derived in this systematic way consistently reaches a value around 0.70 by the end of draw. It is however important to emphasize that as the intensity below the linear background was ignored in the calculation, this orientation parameter does not provide the $< P_2(\cos\theta) >$ parameters of the whole chain segment population and should therefore be regarded as a relative rather than an absolute value of orientation.

Data for the experiments in which the final draw ratio was

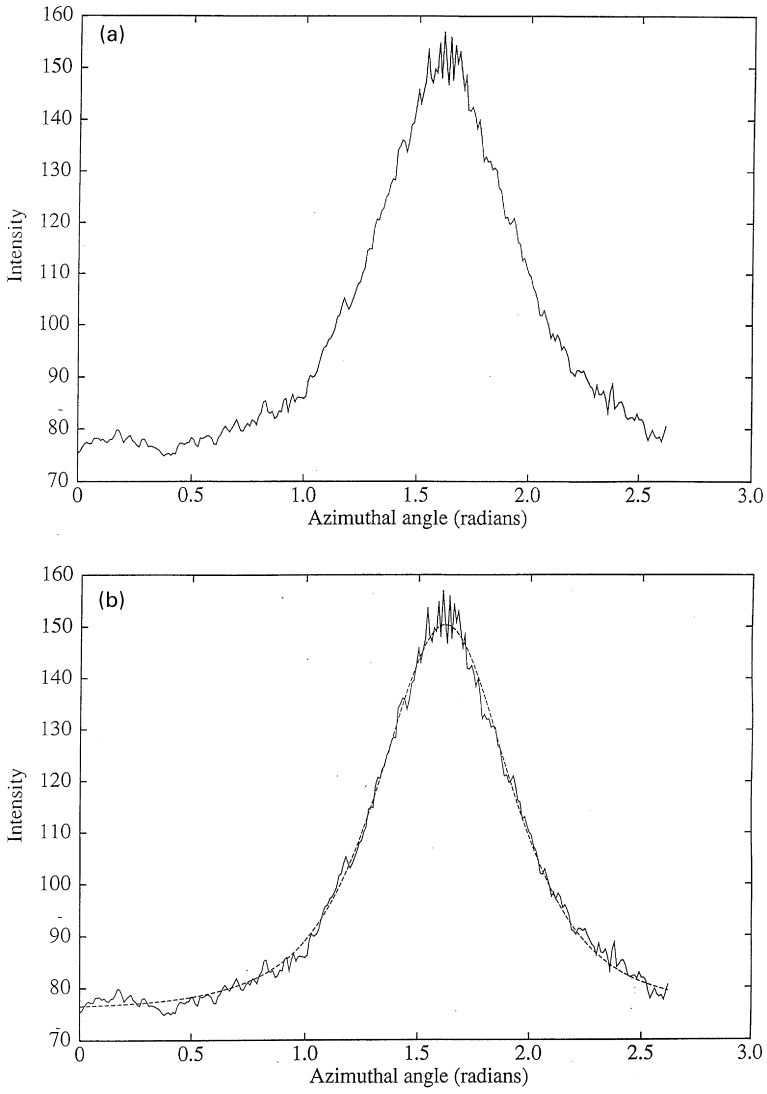

Fig. 6. (a) Azimuthal scan of the equatorial diffraction peak of the diffraction pattern of PET sample drawn at 90°C. (b) Fitting of the azimuthal scan shown by dotted curve.

varied are illustrated in Fig. 8. For each draw ratio, this figure compares the final frame (frame 124) and the frame at completion of the mechanical extension. The patterns in the final frame show the presence of an oriented crystalline phase which decreases in relative intensity with decreasing draw ratio. At a final draw ratio of 2.2:1, the crystalline phase is barely visible and at a draw ratio of 2.0:1 it is not perceptible. The frames corresponding to the end of draw show a progressive decrease in the intensity of the diffuse equatorial lobes with decreasing draw ratio. However it is worth noting that in the case of a draw ratio of 2.0:1, where crystallization does not occur, the equatorial scatter is more intense than in the final frame indicating a relaxation of the molecular segments over the 5 s time scale of the experiment. Fig. 9 shows a plot of the area of the (010) peak determined from scans of the variation in the equatorial intensity together with the variation in the instantaneous draw ratio. This is consistent with the crystallization behaviour being qualitatively the same for all the final draw ratios, in that crystallization begins at the end of the drawing process and then increases asymptotically to a final value. The main difference is that rate of crystallization and the final level of crystallinity decrease with reducing final draw ratio. Fig. 10 shows a plot of the $< P_2(\cos\theta) >$ orientation parameter derived from azimuthal scans. This shows that for draw ratios of $\sim 2.2:1$ and above, the parameter continues to increase after completion of draw as a result of an increased contribution of crystalline reflections to the measured data. However for draw ratios below this, the parameter increases with the drawing process and then falls away within about 25 frames (i.e., 1 s) as soon as the drawing process stops. Once again it is important to emphasize that because of uncertainty in choosing a baseline these parameters should be regarded as relative rather than absolute values.

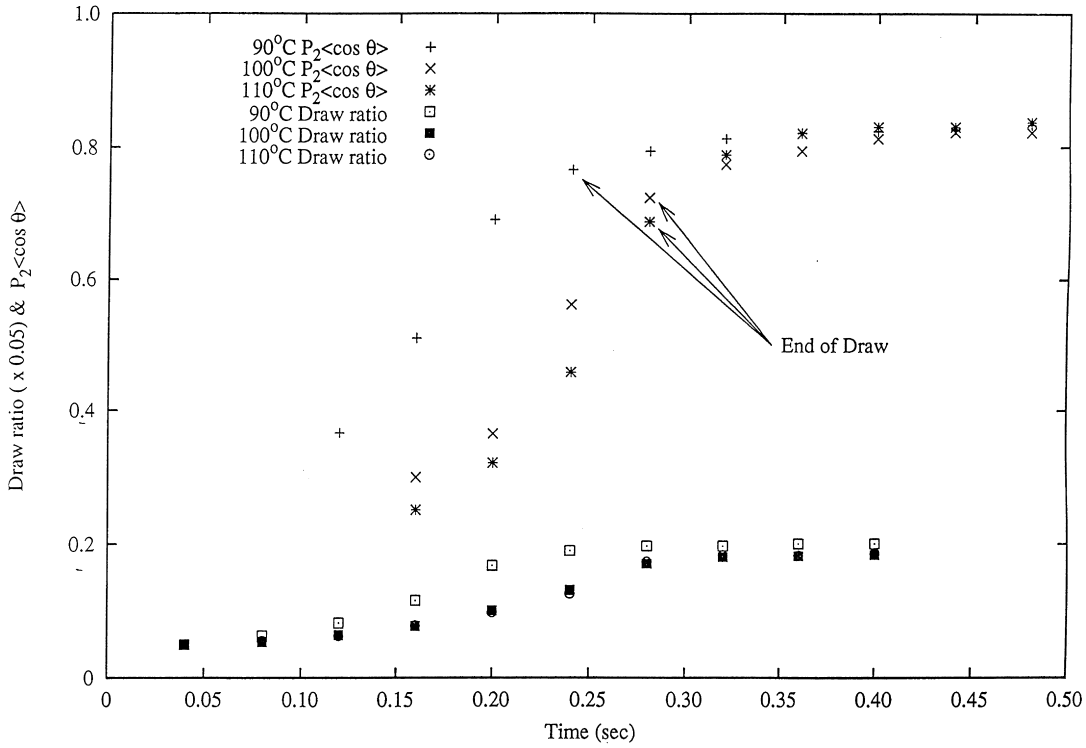

Fig. 7. Plot of draw ratio and the $< P_2(\cos\theta) >$ calculated from the X-ray diffraction pattern of PET samples recorded during drawing at 90°C, 100°C and 110°C for final draw ratio of 4:1. The arrow indicates end of draw.

4. Discussion

4.1. Crystallization regimes

The comparison of X-ray data recorded at this fast draw rate at different draw temperatures (e.g. Fig. 2) clearly shows a change in the crystallization regime, between 125°C and 130°C. Above 125°C, relaxation of the segment orientation is fast enough to prevent conditions suitable for oriented crystallization within the 5 s time scale of the experiment. It is presumed that any crystallization that occurs will be much slower and proceed as in conventional crystallization from an unoriented melt. Separate isothermal measurements on this polymer by DSC in fact show that at 130°C the half-time for conventional crystallization is around 600 s. In contrast the strain-induced crystallization regime occurring below 125°C is clearly quite different and is essentially complete within 1 s.

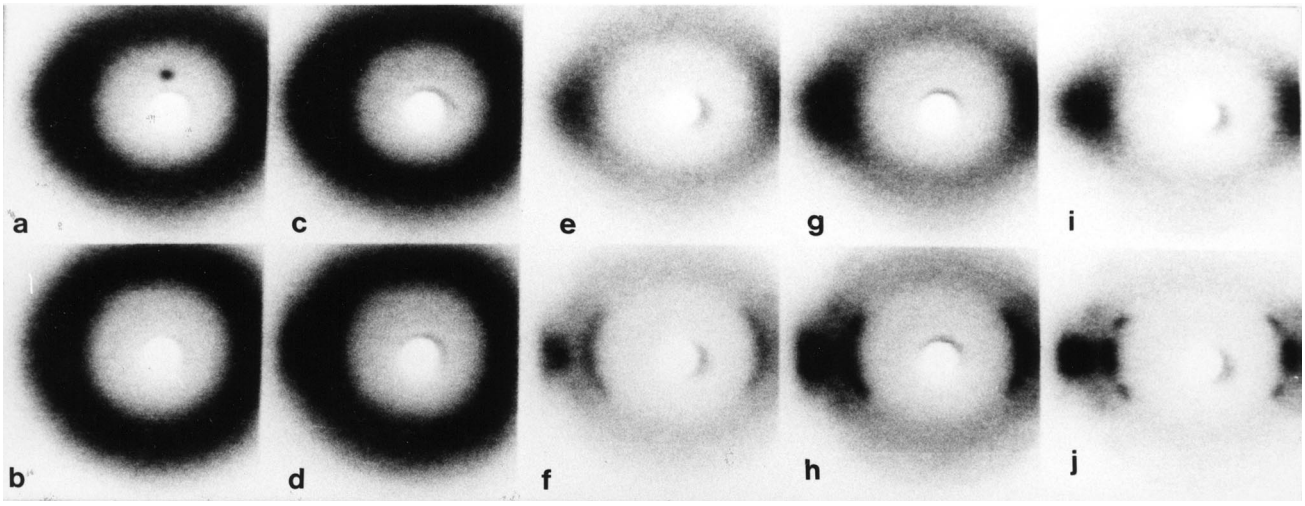

Fig. 8. Sequence of X-ray diffraction patterns of PET sample drawn at 90°C with draw ratios of 2.0 (a, b), 2.2 (c, d), 2.6 (e, f), 3.1 (g, h) and 4.0 (i, j) (i) Diffraction patterns in the top row of the figure (i.e., a, c, e, g and i) corresponding to the end of the draw but before the onset of crystallization. (ii) Diffraction patterns in the bottom row of the figure (i.e., b, d, f, h and j) corresponding to final frame (124) of the experiment.

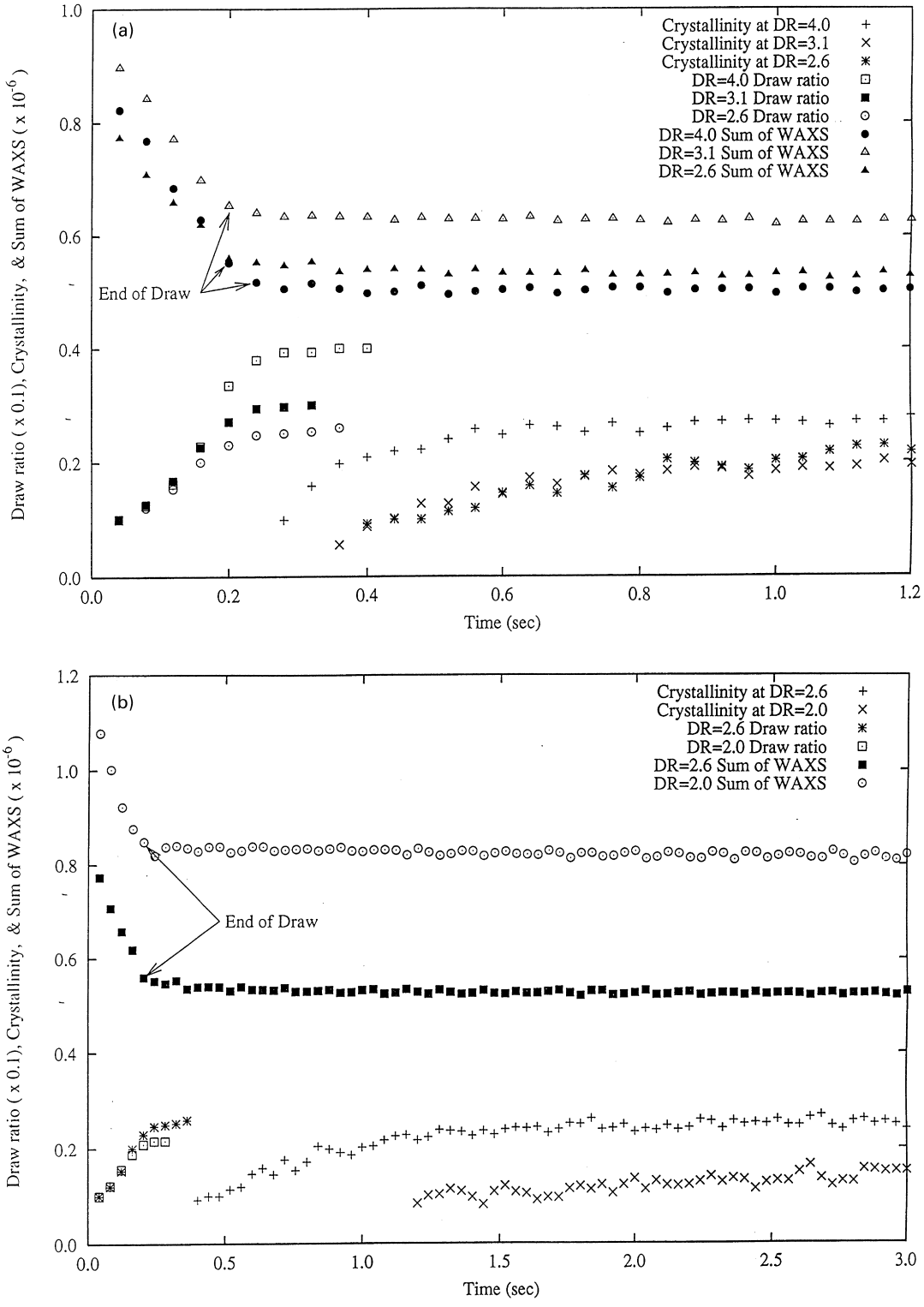

Fig. 9. Variation of crystallinity calculated from the sequence of X-ray diffraction patterns recorded at 90°C for different final draw ratios during the drawing of PET. The arrow indicates the frame with the first detectable crystallinity. (For clarity in Fig. 9 the data for larger draw ratios is plotted in (a) and with some overlap for lower draw ratios in (b))

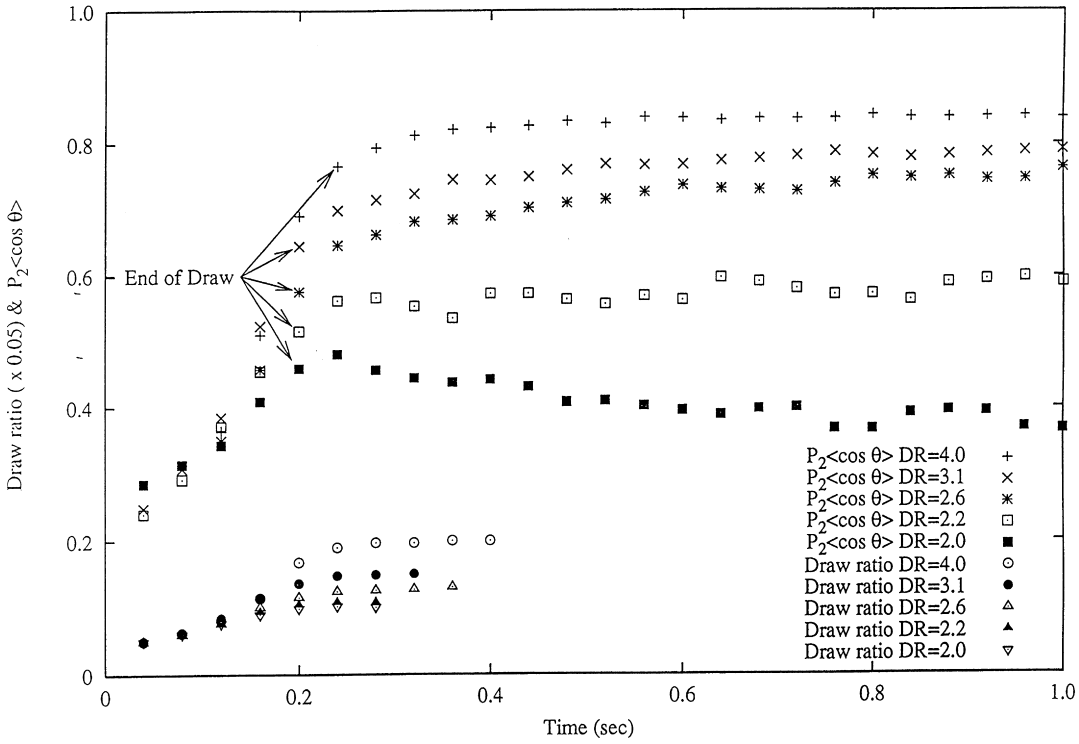

Fig. 10. Variation of $< P_2(\cos\theta) >$ calculated from the sequence of X-ray diffraction patterns recorded at 90°C for different final draw ratios during the drawing of PET. The arrow indicates the end of draw.

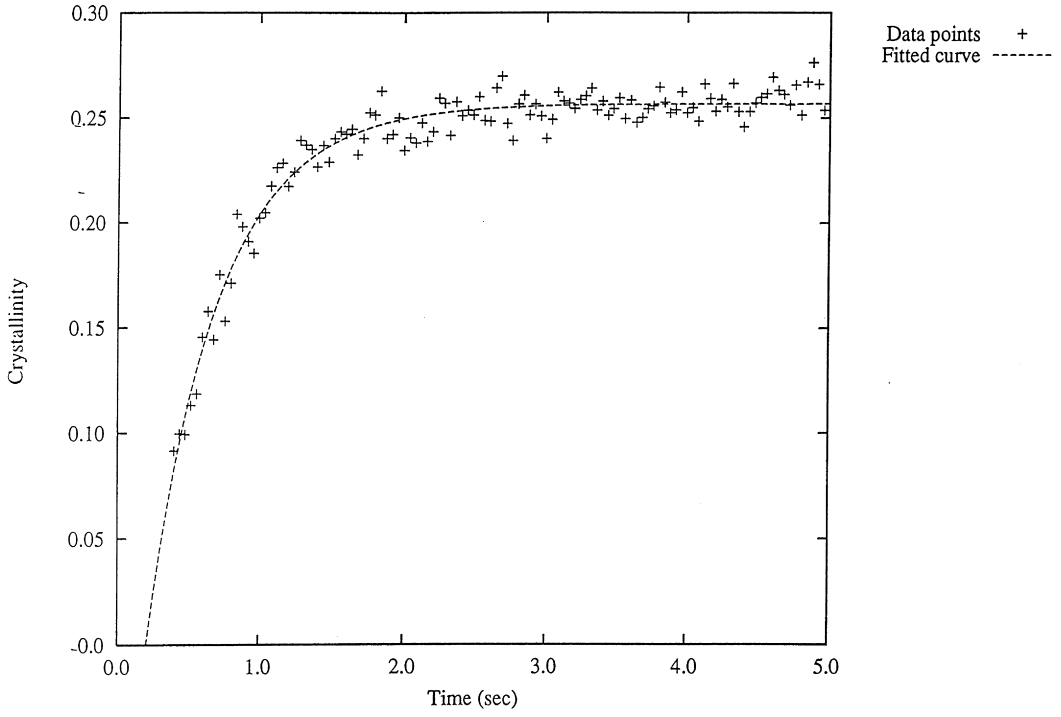

Fig. 11. Plot of the development of crystallinity calculated from the sequence of X-ray diffraction patterns recorded during the drawing of the PET sample at 90°C to a draw ratio of 2.6:1.

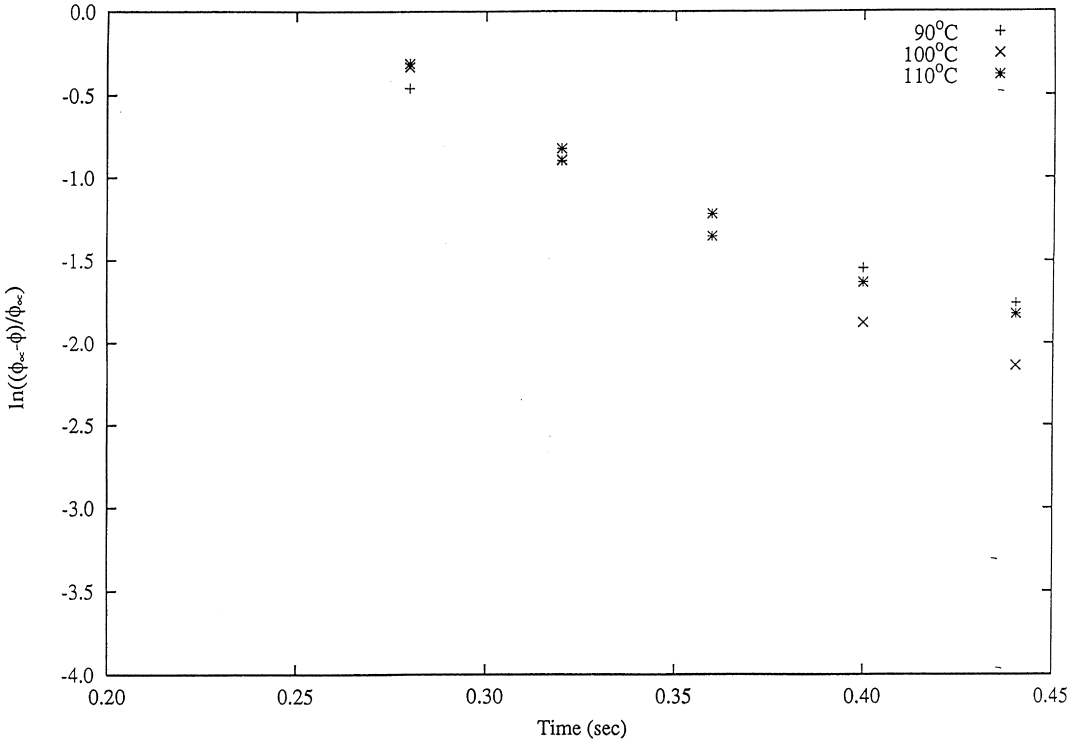

Fig. 12. Logarithmic fit of the development of crystallinity calculated from the sequence of X-ray diffraction patterns recorded during the drawing of PET samples at 90°C, 100°C and 110°C.

4.2. Strain-induced crystallization kinetics

One characteristic feature of the strain-induced crystallization regime at this fast draw rate is that the onset of crystallization does not occur until after the mechanical drawing was completed. This suggests that any attempt by oriented chain segments to move into crystalline register is frustrated by continuing network deformation during the draw process itself. Only when deformation has stopped can the oriented segments cooperatively align to form crystalline lattices. As was recognized in our previous article, the kinetics of the strain-induced regime in which the crystallization asymptotically approaches a limiting value can be appropriately treated in terms of a first order transformation process in which the rate of transformation is proportional to the amount of untransformed phase [1]. First order transformation crystallization kinetics are not unique to the oriented state of PET and have been reported to occur over the same temperature range for crystallization of isotropic PET. Mayhan et al. [9] using light transmission measurements found evidence for first order kinetics in the temperature range 90°C–115°C. They suggested that this zone is associated with the formation of a nucleated intermediate that was distinguishable from the more conventional crystallization that occurs above 120°C, which follows Avrami kinetics with exponents greater than two. Miller [10] observed similar first order kinetics in the same range using more straightforward DSC measurements. However in both these cases the crystallization rate constants were of the order of $10^{-3}\,s^{-1}$ and are four orders of magnitude slower than the oriented crystallization observed here. In order to characterize the crystallization in terms of a first order transformation process, the data was examined using the relationship:

$$(\phi_\infty - \phi)/\phi_\infty = e^{-kt} \quad (1)$$

where ϕ_∞ represents the final attained crystallinity, ϕ is the crystallinity after time, t, from the start of the crystallization process and k is a rate parameter. The crystalline peak area measurements from the complete set of 124 frames in each draw experiment were be tested against these kinetics by carrying out a least squares fit to Eq. (1) in which ϕ_∞ and k were unconstrained. The problem with performing this on a large data set, where most of the crystallinity change occurs within the first few data points and where there is a significant degree of noise, is that the fit becomes insensitive to k and hence does not capture the essential shape of the kinetics. However in the experiments at lower draw ratios, where the crystallization is slower, a full direct fit becomes more appropriate for assessing the validity of these kinetics. Fig. 11 shows an example of a fit for an experiment at a draw ratio 2.6:1, where it can be seen that the crystallization process very closely follows first order kinetics. The extrapolation to zero crystallization coincides closely with end of draw shown in Fig. 9. Alternatively the data can be tested by plotting $\ln\{(\phi_\infty - \phi)/\phi_\infty\}$ against t, where one would expect a linear relationship with a slope of $-k$. Fig. 12 shows such

plots using the first few data points for the series of variable temperature experiments where the crystallization was faster. Because of the difficulty of judging the final asymptotic behaviour, various test values of ϕ_∞ were taken close to the final asymptote to establish reasonable linear relationships over the majority of the data points. Different trial values for ϕ_∞ had a very minor effect on the initial data points but did allow a choice where more points conformed to the main trend. The plots are sufficiently linear to show that the first order analysis is a reasonable approach. However in view of the noise and uncertainties in the data points the fit is less convincing than in Fig. 11 where the shape is better resolved.

Within the uncertainties of the data points, the slopes are all similar to within about 10% and correspond to a rate constant, k, of $\sim 10\ s^{-1}$. The insensitivity of the rate to temperature implies a very low apparent activation energy of ~ 1 kcal/mole/K or less. This is in contrast to the work of Mayhan et al.[9] and Miller [10] on unoriented PET who found activation energies around ~ 40 kcal/mole/K. The same first order kinetics in this temperature range for both unoriented and oriented cases could imply similarity in the nature of the nucleated crystal species being formed as discussed in more detail below. The much faster rate and the much lower activation energy could be as a result of oriented chain segments having less hindrance in moving into crystal register. As suggested previously, the very low activation energy in the oriented case indicates that the rate of the crystallization process is governed by the mobility of local chain segments rather than the transport of chain motions associated with the glass transition. Alternatively the insensitivity with temperature for the overall observed crystallization process could be the result of more than one factor where there are opposing temperature effects. It is worth noting that Sun et al. [11] report evidence of a systematic decrease in activation energy with increasing orientation.

4.3. Segment orientation of deformed chain network

In both the variable draw ratio and variable temperature experiments, the oriented crystallization process was preceded by the appearance of diffuse equatorial lobes in the diffraction pattern. It is reasonable to attribute this diffraction feature to inter-chain scattering and to expect the maximum to be in the direction that is mutually perpendicular to adjacent segments of neighbouring chains. As PET comprises fairly rigid terephthalate residues, this diffraction will be predominantly perpendicular to the main axis of these residue segments. The azimuthal distribution of intensity of the lobes will therefore approximately represent the distribution of chain segments around the draw direction.

The results indicate that the presence of these oriented, non-crystalline segments is a key element that enables the fast oriented crystallization to occur. For example, as is demonstrated in Fig. 2, oriented crystallization does not occur above 125°C, where the oriented segment component is not detected. Also, in the experiments at 90°C shown in Fig. 8, both the rate and level of crystallization decrease with decreasing amount of this component, as the draw ratio is reduced. In this respect the results for draw ratio ~ 2.0:1 are particularly interesting as they give direct information on the stability of the oriented component. This shows that at 90°C, in the absence of crystallization, the most highly oriented component decays by relaxation of the segments at a rate of the order of $\sim 2\ s^{-1}$. All these results are consistent with the prerequisite that at each drawing condition, oriented crystallization depends on the presence of a sufficient quantity of the highly oriented segments. If the rate of nucleation/crystallization is not significantly faster than the decay of the oriented segments then the oriented crystallization will not occur.

It is envisaged that the oriented segment population forms when the network of entangled chains in the initially unoriented polymer is stretched at a rate that is faster than the reptation rate and possibly faster than the dynamics of the main Rouse modes of the chains. As such the deformed network will be far from an equilibrium structure and will result in sequences of oriented segments stretched out predominantly in the draw direction. When the mechanical drawing ceases in the absence of crystallization, the segmental motions will enable the network of chains to move towards equilibrium. In the first instance the chains between entanglements will move towards random configurations, and over a longer time scale the entanglements will relax by reptation, returning towards an isotropic state. However the mobility of the segments also allows them to undergo mutual alignment and thus potentially to nucleate crystal lattices which will arrest relaxation of the overall orientation.

The first order kinetics described are consistent with a sporadic transformation of localized oriented segments into crystals which would continue to occur randomly in space until the source of oriented segments is exhausted or further mobility is restricted by the growing number of nucleated crystals creating “cross links” which freeze motion in their neighbourhood. In principle this only requires the extended oriented segments to be initially randomly arranged in space and does not require them to form a phase separated from other chain configurations. However a view has been expressed that oriented PET can also exist in a mesomorphic form [12–16]. The diffuse equatorial spots seen in Figs. 2 and 8 just before crystallization occurs are in fact similar to those cited for the mesomorphic form but other defining features characteristic of this form are unfortunately not resolvable in the patterns. However it should be noted that an analysis by Auriemma et al. [15] was unable to demonstrate the necessity for a distinct separated mesophase and showed that the pattern could be accounted for by extended linear chains of random monomeric sequences with no long range correlation

between planes of phenyl rings. However by analogy with the recent studies of Keller and co-authors[17] on polyethylene, the concept of a mesophase may still be valid as an intermediate state between randomly arranged extended chain sequences and the final crystals. We hope to be able to clarify this issue in related studies we are currently undertaking.

4.4. Comparison with interrupted draw data

This new set of data demonstrates for the fast draw rates used in this work that the observation that crystallization does not start until after completion of the drawing process also holds for lower final draw ratios down to $\sim$ 2.0:1. This clearly demonstrates the problem of relying on data from interrupted draw experiments to deduce the instantaneous crystallinity during the fast drawing of PET. In order to carry out an ideal interrupted draw experiment it is necessary to quench the sample below T_g while still in the clamps and before any change in crystallization occurs. The time necessary to do this in practice will be limited by the heat transfer from the sample and its thermal diffusivity. For most reasonable sized samples this time scale is likely to be comparable or significantly longer than the time scale of the crystallization observed in the present experiments [1]. Thus any observation of crystallinity will depend on whether or not the quenching rate in the experiment is faster than the strain-induced crystallization experiment. The apparent onset of crystallinity deduced from interrupted draw experiments will correspond to the draw ratio at which the crystallization rate becomes comparable to the quenching rate. The only way of preserving the oriented non-crystalline state would be to use very thin samples that can be efficiently cooled. An example of this would be the samples described by Napolitano et al. [14] and Nicholson et al. [16] in which yarn was drawn continuously followed by rapid cooling with air jets.

5. Conclusions

These experiments with varying temperature and draw ratio have illustrated two of the bounds of the regime within which oriented crystallization occurs during the fast drawing of PET. The increasing chain mobility with temperature allows chain relaxation to compete with the deformation of the drawing force until above a critical upper temperature bound of 125°C where no oriented crystallization could be detected. With decreasing final draw ratio at 90°C, both the rate of crystallization and the final level of crystallinity decrease with decreasing amount of oriented segments until, below a lower critical draw ratio of $\sim 2:1$, the oriented segments relax at a rate which is faster than crystallization can occur. Both bounds demonstrate the requirement to generate an adequate level of extended chain segments. The data for draw ratio $\sim 2.0:1$ shows these chain segments relaxing their orientation at a rate of $\sim 2\ s^{-1}$.

The oriented crystallization appears to follow the kinetics of a first order transformation process. Within the experimental error, there was no significant change in rate between 85°C and 110°C. This indicates a very low apparent activation energy and could suggests the process is only limited by local segment mobility rather than main chain motions; alternatively the insensitivity to temperature could be as a result of competing processes with opposing temperature effects. A suitable model for the process would be that of the oriented chain segments undergoing local motions to align in crystallographic register to sporadically form crystal nuclei. Within experimental error the oriented crystallization process did not commence until after the completion of the mechanical draw process. The discrepancy with data from interrupted draw experiments of previous authors where the crystallization is deduced to occur during the drawing process can probably be explained in terms of the quenching rate of the experiments not being faster than the crystallization rate.

Acknowledgements

This work was supported by the allocation of beam time at the ESRF. We are grateful to M. Daniels, M. G. Davies, G. Dudley, E. J. T. Greasley, G. Marsh, M. Wallace and C. Sutton for technical support and help with preparation of the manuscript.

References

[1] Blundell DJ, MacKerron DH, Fuller W, Mahendrasingam A, Martin C, Oldman RJ, Rule RJ, Riekel C. Polymer 1996;37:3303.
[2] Salem DR. Polymer 1992;33:3182.
[3] Le Bourvellec G, Monnerie L. Polymer 1986;27:856.
[4] Mahendrasingam A, Fuller W, Forsyth VT, Oldman RJ, MacKerron DH, Blundell DJ. Rev Sci Instrum 1992;63:1087.
[5] Casey M. Polymer 1977;18:1219.
[6] Daubeny Rde P, Bunn C, Brown CJ. Proc R Soc London Ser 1954;A 226:531.
[7] Hall MM, Veeraraghavan VG, Rubin H, Winchell PG. J Appl Cryst 1977;10:66.
[8] Lovell R, Mitchell GR. Acta Cryst 1981;A37:135.
[9] Mayhan KG, James WJ, Bosch W. J Appl Polymer Sci 1965;9:3605.
[10] Miller B. J Appl Polymer Sci 1967;11:2343.
[11] Sun T, Pereira T, Porter RS. J Polymer Sci (Polymer Phys Ed) 1984;22:1163.
[12] Bonart R. Kolloid-Z 1966;213:1.
[13] Linder WL. Polymer 1973;14:9.
[14] Napolitano MJ, Moet AJ. J Appl Polymer Sci 1987;34:1285.
[15] Auriemma F, Corradini P, de Rosa C, Guerra G, Petraccone V, Bianchi R, di Dino G. Macromolecules 1992;25:2490.
[16] Nicholson TM, Davies GR, Ward IM. Polymer 1994;35:4259.
[17] Keller A. In: Dosiere M, editor. Crystallisation of polymers. NATO Advanced Research Workshop, Mons, Belgium, 1992.